EUROPEAN ORGANIZATION FOR NUCLEAR RESEARCH

L3 note 1807
12-07-95

A Study of Initial State Photon Radiation in the Reaction $e^+e^- \to \mu^+\mu^-\gamma$

L3 Collaboration

Abstract

Using the data recorded with the L3 detector at LEP we study the effect of initial state radiation in the process $e^+e^- \to \mu^+\mu^-\gamma$. The data sample corresponds to an integrated luminosity of 119 pb^{-1} and yields 225 muon pair events with missing momentum along the beam direction. They are interpreted as events with a hard initial state photon. The effective center of mass energies of the outgoing muons range from 50 to 85 GeV. The events are used to determine the cross section and to measure the forward-backward asymmetry below the Z resonance.

Submitted to EPS and Lepton-Photon Conferences in July 1995

1 Introduction

At LEP the cross sections and asymmetries for the process $e^+e^- \to f\bar{f}(\gamma)$ are measured at center-of-mass energies between 88 and 94 GeV [1]. Data from experiments at PEP, PETRA and TRISTAN cover the energy range from 10 to 60 GeV [2]. The energy region not yet explored by direct measurements can be accessed at LEP using events with hard initial state photon radiation, in which the fermion pair is produced at lower center of mass energies.

The following analysis uses muon pair events collected with the L3 detector from 1991 to 1994. The data correspond to an integrated luminosity of 119 pb^{-1}. Events with high missing momentum along the beam direction are interpreted as events with hard initial state photon radiation. They are used to measure cross sections and asymmetries between 50 and 85 GeV.

2 Photon Radiation in Fermion Production

QED corrections to the process $e^+e^- \to f\bar{f}(\gamma)$ can be separated into initial and final state radiation and their interference. The initial state radiation has a large influence on the cross sections and asymmetries, whereas the contribution from the final state photon radiation is small [3]. For center of mass energies around the Z resonance the final lifetime of the Z boson decouples initial and final state radiative effects and suppresses their interference [4]. This holds as long as no strong kinematical cuts are applied.

In the process of initial state bremsstrahlung a fraction of the beam energy is carried away by the photon and the fermion pair is produced at a lower center-of-mass energy, $\sqrt{s'}$. The visible cross section is described by a convolution of the Born cross section with a radiator function, $G(z)$,

$$\sigma(s) = \int_{4m_f^2/s}^{1} dz\; G(z)\; \sigma_{Born}(zs)\;,$$

where $z = s'/s$. The differential cross section of initial state photon radiation is then given by the product of the radiator function and the Born cross section itself:

$$\frac{d\sigma}{dz} = G(z)\; \sigma_{Born}(s')\;.$$

A first order calculation for hard photon radiation leads to [5]

$$G(z) = \frac{\alpha}{\pi}\,(L-1)\,\frac{1+z^2}{z-1}\;,$$

where $L = \ln s/m_e^2$ can be assumed constant at LEP energies. From the energy of the initial state photon one finds for s':

$$s' = s\left(1 - 2\frac{E_\gamma}{\sqrt{s}}\right) . \tag{1}$$

Since photons are predominately emitted collinear to the direction of the radiating particle, initial state photons mostly go along the direction of the beams while final state photons cover the full solid angle. Thus a separation of the different radiation types and the determination of s' is possible.

For three particle final states the directions of the particles fix their momenta. Here we assume that the undetected initial state photon was radiated in the direction of the beams. Then the photon energy is given by the polar angles of the outgoing fermions:

$$E_\gamma = \sqrt{s}\,\frac{|\sin(\theta_1+\theta_2)|}{\sin\theta_1 + \sin\theta_2 + |\sin(\theta_1+\theta_2)|} . \tag{2}$$

In the presence of additional photons in the final state relation 2 cannot be applied.

In this analysis we use events of the reaction $e^+e^- \to \mu^+\mu^-\gamma$. They allow a clear separation between photons and outgoing leptons and thus a rejection of the final state bremsstrahlung events. Moreover the polar angles of the two leptons can be measured with good precision, which is necessary for the determination of s'.

We use fully simulated and reconstructed muon pair events generated with the KORALZ 3.8 [6] program to compare the photon energy calculated according equation (2) with the generated value. The resolution for the energy of the initial state photon is 5 % and shown in figure 1. Formula (1) gives the reduced center of mass energy $\sqrt{s'}$ for the $\mu\mu$ system. Figure 2 shows the calculated $\sqrt{s'}$ compared to the one we expect from the generated photon energy. The resolution of $\sqrt{s'}$ is found to be 430 MeV.

3 Event Selection

Our event selection for muon pair production [1], $e^+e^- \to \mu^+\mu^-(\gamma)$, requires two muon tracks reconstructed in the L3 muon chambers or one muon track and the signature of a minimal ionizing particle in the inner detector parts. One of the muons has to be within the fiducial angular region of $|\cos\theta_\mu| < 0.8$, the other inside $|\cos\theta_\mu| < 0.95$. To remove cosmic background we ask for a hit in the scintillation counters within a ± 3 ns time window around the beam crossing. In addition, at least one of the muons must have a track in the inner tracking chamber with a distance of less than 5 mm to the nominal vertex. Hadronic Z decays are rejected by asking a calorimetric cluster multiplicity of less than 15.

For the accepted events we apply equation (2) to calculate the energy of the initial state photon, E_γ. As we are interested to study events, where the center of mass energy of the $\mu\mu$ system is reduced, we require $\sqrt{s'}$ to be lower than 95% of $\sqrt{s}$.

We calculate the fraction between the momentum of the most energetic muon, p_{max}, and the energy, which is left for the muon system, $\sqrt{s} - E_\gamma$. The distribution of this fraction is shown in figure 3 for data and Monte Carlo. The background sources are the reaction $e^+e^- \to \tau^+\tau^-$ and the four fermion production, $e^+e^- \to e^+e^-\mu^+\mu^-$, where both final state electrons stay undetected in the beam pipe. The cut $p_{max} > 0.4(\sqrt{s} - E_\gamma)$ removes most of the background.

Figure 4 shows for simulated events a comparison between the reconstructed photon energy, $E_{\gamma rec}$, and the generated energy of the photon, $E_{\gamma gen}$. For events, where the photon was emitted along the beams, the method to determine E_γ from the muon angles reproduces well the generated photon energy (region A). For the events of region B a large photon energy is reconstructed, although no photon parallel to the beam is present. A part of these events shows hard photon radiation away from the beam direction, others are affected by a misreconstruction of the muon polar angles.

In the following the events of region B are considered as background for our event selection. They are removed by the following cuts:

- The acoplanarity of the muons is required to be less than 2°. The distribution of this quantity is shown in figure 5. Events with an initial state photon are distributed at $|\Delta\Phi_\mu - 180°| = 0°$.

- We cut on the energy deposit in the electromagnetic calorimeter. For the electromagnetic clusters we calculate the energy fraction perpendicular to the direction of the nearest muon, E_{trans}. The distribution of E_{trans} is shown in figure 6. We accept the event, if no cluster with E_{trans} larger than 1.5 GeV is found. To allow final state photon rejection outside the acceptance region of the electromagnetic calorimeter, a cut on the energy measured by the hadron calorimeter is applied.

- The polar angle of the muon is measured with the z-chambers of the muon spectrometer. We verify this measurement by comparing it to the polar angle determination using the calorimeters. Figure 7 shows the difference of the two polar angles. If the measurements differ by more than 2°, we reject the event.

From the Monte Carlo with full detector simulation we determine the efficiency, ϵ_{eff}, to select radiative muon pair events inside the fiducial volume of our selection, $|\cos\theta_\mu|_{max} < 0.95$, $|\cos\theta_\mu|_{min} < 0.8$, $|\cos\theta_\gamma| > 0.98$ and $|\Delta\Phi_\mu - 180°| < 2°$. We use Monte Carlo events on generator level to perform the extrapolation to the full phase space. The resulting acceptances, ϵ_{acp}, together with the detector efficiencies, ϵ_{eff}, are given in table 1.

Table 2 gives the background contributions from the reactions $e^+e^- \rightarrow \tau^+\tau^-$ and $e^+e^- \rightarrow e^+e^-\mu^+\mu^-$ as predicted by Monte Carlo. Additionally we quote the contamination from muon pair events with no photon radiation along the beam, $\eta_{\mu\mu}$. We use a Monte Carlo study on generator level to determine the fraction of our selected radiative events which is due to final state bremsstrahlung.

Out of all events recorded in the years 1991 to 1994 ($\mathcal{L}$ = 119 pb^{-1}) we select 225 $e^+e^- \rightarrow \mu^+\mu^-\gamma_{isr}$ candidates with a center-of-mass energy of the muon pair of less than 85 GeV. The $\sqrt{s'}$ distribution for the selected events is shown in figure 8.

$\sqrt{s'}$[GeV]	ϵ_{eff}[%]	ϵ_{acp}[%]
50 - 64	43.0 ± 4.8	51.0 ± 0.8
64 - 76	72.6 ± 3.6	57.4 ± 0.6
76 - 82	73.1 ± 2.9	57.7 ± 0.6
82 - 85	82.4 ± 2.2	59.5 ± 0.5

Table 1: Detector efficiencies, ϵ_{eff}, and acceptances, ϵ_{acp}, of our selection

$\sqrt{s'}$[GeV]	$\eta_{\tau\tau}$[%]	$\eta_{ee\mu\mu}$[%]	$\eta_{\mu\mu}$[%]	η_{fsr}[%]
50 - 64	< 6.3	1.1 ± 0.3	< 2.1	3.6 ± 0.4
64 - 76	< 2.5	1.1 ± 0.3	1.3 ± 0.9	7.5 ± 0.4
76 - 82	3.0 ± 2.1	< 0.2	0.8 ± 0.6	8.7 ± 0.4
82 - 85	2.0 ± 1.4	< 0.1	1.3 ± 0.6	8.1 ± 0.3

Table 2: Background contribution from the processes $e^+e^- \rightarrow \tau^+\tau^-$ ($\eta_{\tau\tau}$), $e^+e^- \rightarrow e^+e^-\mu^+\mu^-$ ($\eta_{ee\mu\mu}$), $e^+e^- \rightarrow \mu^+\mu^-$ ($\eta_{\mu\mu}$) and the contamination from final state events (η_{fsr}).

4 Determination of the Cross Section

For the cross section measurement only events from runs at the Z peak are used. Table 3 lists the number of selected $e^+e^- \rightarrow \mu^+\mu^-\gamma_{isr}$ events for the different $\sqrt{s'}$ bins. The events correspond to a total luminosity of 88 pb^{-1}.

We use the KORALZ Monte Carlo to predict the number of selected events for a given $\sqrt{s'}$ bin. A comparison to data tests the convolution of equation (2) and in particular the energy dependent cross section used by the Monte Carlo program.

Assuming that the initial state photon radiation is described correctly by the Monte Carlo, the ratio between the number of events seen in data and the number predicted by the simulation can be interpreted as a cross section:

$$\sigma_B^{meas}(\langle\sqrt{s'}\rangle) = \sigma_B^{theo}(\langle\sqrt{s'}\rangle)\frac{N_{sel}(1-\eta)}{N_{exp}}$$

Here $\langle\sqrt{s'}\rangle$ is the mean $\sqrt{s'}$ value of the data in the corresponding energy bin.

The resulting Born cross sections for the four different energy points are listed in Table 3. The quoted systematic error is due to Monte Carlo statistics and background subtraction.

Figure 9 shows the calculated cross section in comparison to the lowest order Standard Model prediction. We include the results obtained by L3 for $\sqrt{s}$ values around the Z mass [1]. The measurements are corrected for bremsstrahlung and electroweak radiative effects. The correction is determined by comparing the analytical program ZFITTER 4.6 [7] to the lowest order Born prediction. In addition we show the results of the muon cross section measured in the energy range between 10 and 60 GeV at PETRA, PEP and TRISTAN [2]. Over the full energy range the measurements are in agreement with the Standard Model prediction. The data of this analysis provide additional points between the TRISTAN and the LEP energies.

$\sqrt{s'}$[GeV]	$\langle\sqrt{s'}\rangle$[GeV]	N_{sel}	σ_{Born} ±(stat.)±(syst.) [pb]
50 - 64	57.2	11	$25.4 \pm 7.7 \pm 4.3$
64 - 76	72.2	41	$31.8 \pm 5.0 \pm 3.2$
76 - 82	79.6	49	$35.7 \pm 5.1 \pm 2.8$
82 - 85	83.8	75	$67.9 \pm 7.9 \pm 4.3$

Table 3: Number of selected events, N_{sel}, and resulting Born cross section, σ_{Born}.

5 Forward Backward Asymmetry

At Born level the differential cross section of the muon pair production is parameterized by the total cross section, σ_{tot}, and the forward backward asymmetry, A_{FB}:

$$\frac{d\sigma}{d\cos\theta^*} = \sigma_{tot}\left(\tfrac{3}{8}(1+\cos^2\theta^*) + A_{FB}\cos\theta^*\right) .$$

Here θ^* is the polar angle of the μ^- in the center of mass system of the muon pair. For events boosted along the beam direction θ^* can be calculated from the muon polar angles θ_{μ^-} and θ_{μ^+}:

$$\cos\theta^* = \frac{\sin(\theta_{\mu^+} - \theta_{\mu^-})}{\sin\theta_{\mu^+} + \sin\theta_{\mu^-}} .$$

The forward backward asymmetry is then determined by an unbinned likelihood fit, where the likelihood L is defined as the product of the single event probabilities:

$$L = \prod_i \left(\tfrac{3}{8}\,(1+\cos^2\theta_i^*) + A_{FB}\cos\theta_i^* \right) .$$

The asymmetries we measure in the different $\sqrt{s'}$ regions, corrected for the background contamination, are given in table 4. The background from events with final state radiation is mainly located at small and large values of θ^*. The weight of these events in the asymmetry determination is therefore larger than the values one would expect from the event fraction only. Our background subtraction accounts for this effect. The uncertainty of the background from other reactions is the main source of the systematic uncertainty.

Figure 10 shows our results, corrected for electroweak radiative effects, together with the L3 measurements around the Z peak [1] and the forward backward asymmetries obtained by the experiments at PETRA, PEP and TRISTAN [2]. The L3 asymmetry values which were measured on the resonance are corrected for the effect of bremsstrahlung and electroweak radiative corrections. The data are compared to the lowest order Born prediction.

$\sqrt{s'}$[GeV]	$\langle\sqrt{s'}\rangle$[GeV]	N_F	N_B	A_{FB} ±(stat.)±(syst.)
50 - 64	56.7	5	9	$-0.09 \pm 0.32 \pm 0.07$
64 - 76	72.2	12	36	$-0.64 \pm 0.14 \pm 0.03$
76 - 82	79.6	17	40	$-0.59 \pm 0.15 \pm 0.02$
82 - 85	83.8	37	69	$-0.43 \pm 0.11 \pm 0.02$

Table 4: Measured forward backward asymmetry, A_{FB}, corrected for the background contamination.

6 Conclusion

The effect of initial state radiation in the process $e^+e^- \rightarrow \mu^+\mu^-(\gamma)$ is studied. We select 225 events with a hard initial photon and use them to measure cross sections and asymmetries below the Z resonance. Our results show agreement with the Standard Model prediction.

References

[1] L3 Collab., M. Acciarri *et al.*, Z. Phys. **C 62** (1994) 551.

[2] HRS Collab., M. Derrick *et al.*, Phys. Rev. **D 31** (1985) 2352;
MAC Collab., W.W. Ash *et al.*, Phys. Rev. Lett. **55** (1985) 1831;
MARK II Collab., M.E. Levi *et al.*, Phys. Rev. Lett. **51** (1983) 1941;
CELLO Collab., H.-J. Behrend *et al.*, Phys. Lett. **B 191** (1987) 209;
JADE Collab., W. Bartel *et al.*, Z. Phys. **C 26** (1985) 507;
MARK J Collab., B. Adeva *et al.*, Phys. Rev. **D 38** (1988) 2665;
PLUTO Collab., Ch. Berger *et al.*, Z. Phys. **C 21** (1983) 53;
TASSO Collab., W. Braunschweig *et al.*, Z. Phys. **C 40** (1988) 163;
AMY Collab., A. Bacala *et al.*, Phys. Lett. **B 218** (1989) 112;
TOPAZ Collab., B. Howell *et al.*, Phys. Lett. **B 291** (1992) 206;
VENUS Colab., K. Abe *et al.*, Z. Phys. **C 48** (1990) 13.

[3] F.A. Berends, R. Kleiss and S. Jadach, Nucl. Phys. **B 202** (1982) 63.

[4] S. Jadach and Z. Wąs, Phys. Lett. **B 219** (1989) 103.

[5] F.A. Berends, W.L. van Neerven and G.J.H. Burgers, Nucl. Phys. **B 297** (1988) 429.

[6] S. Jadach, B.F.L. Ward and Z. Wąs, Comp. Phys. Comm. **66** (1991) 276.

[7] D. Bardin *et al.*, FORTRAN package ZFITTER, and preprint CERN–TH. 6443/92.

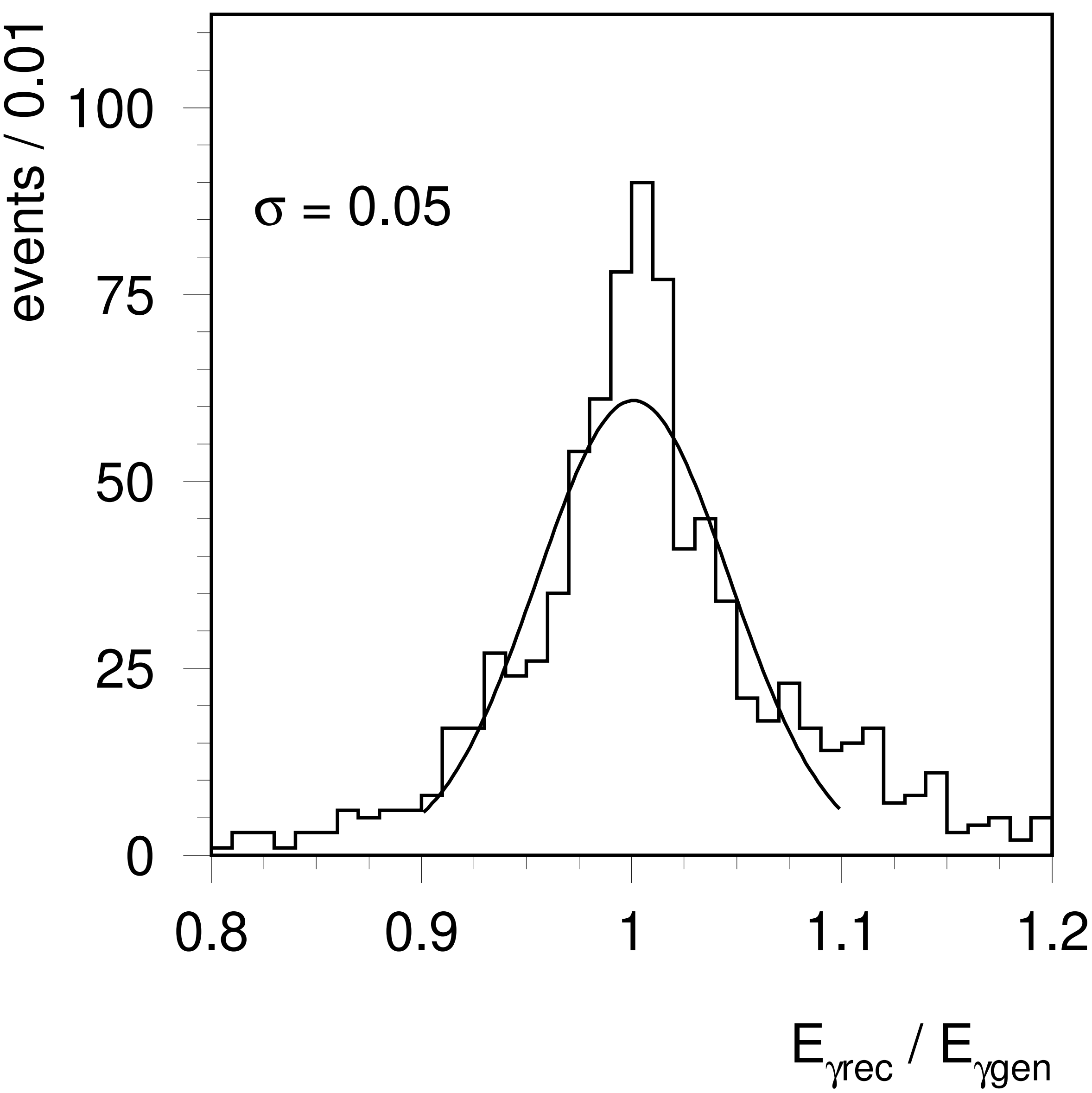

Figure 1: Resolution of the energy of the initial state photon, E_γ, for Monte Carlo events.

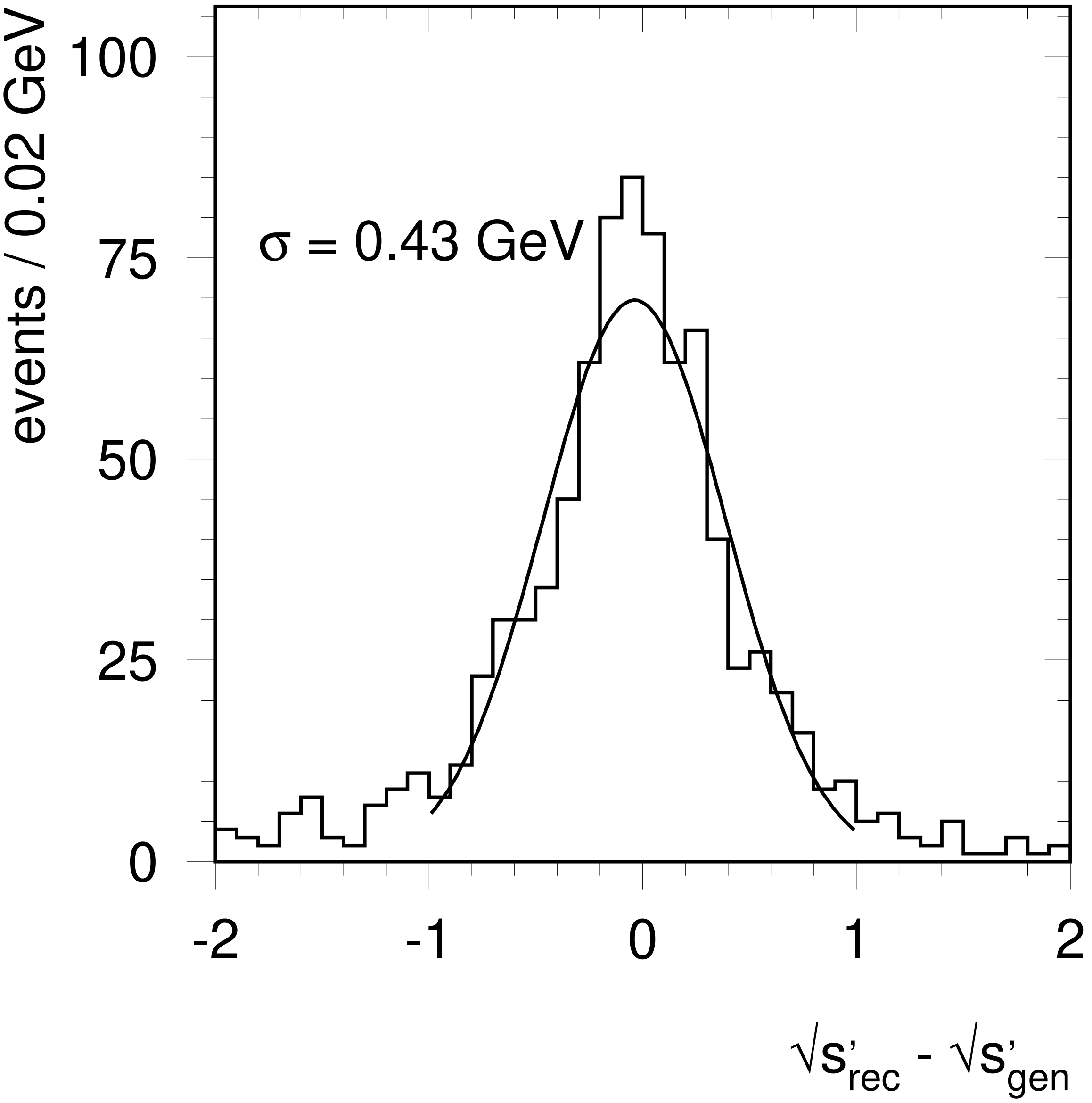

Figure 2: Resolution of the reconstructed $\sqrt{s'}$ for Monte Carlo events.

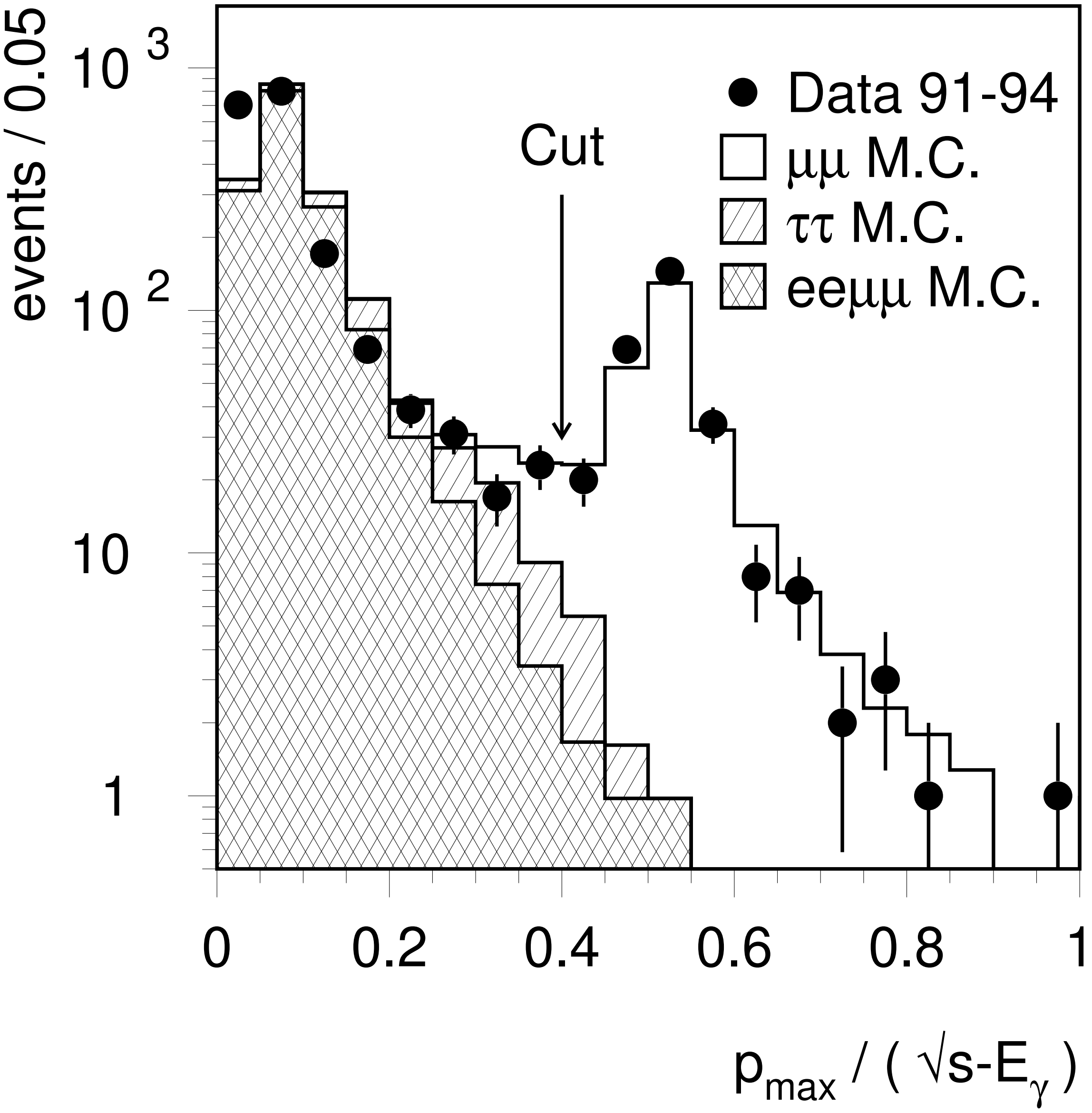

Figure 3: Normalized maximal muon momentum for data, signal and background Monte Carlo.

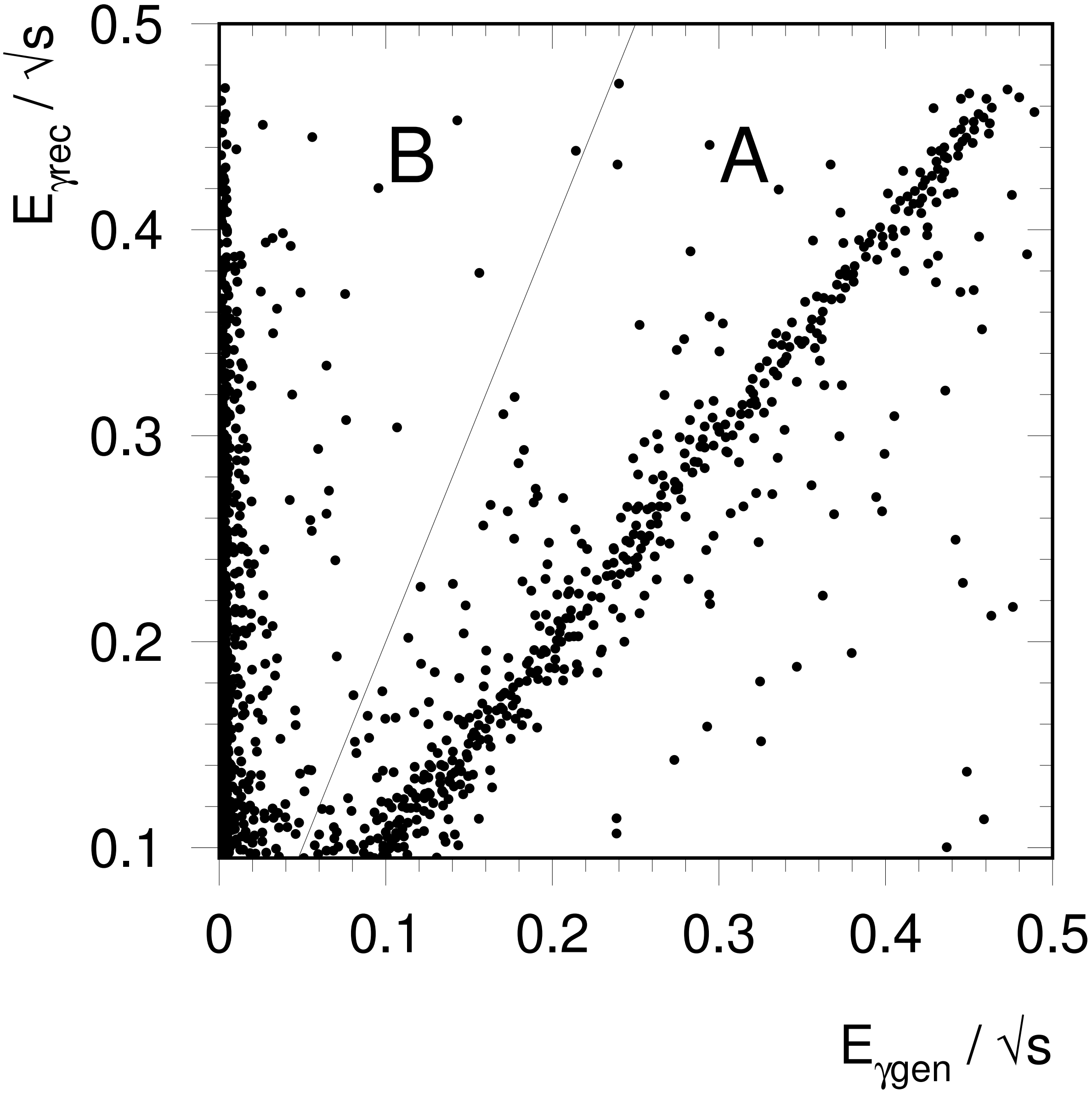

Figure 4: Reconstructed photon energy, $E_{\gamma rec}$, caculated by using formula (2), compared to the generated photon energy, $E_{\gamma gen}$, for Monte Carlo events.

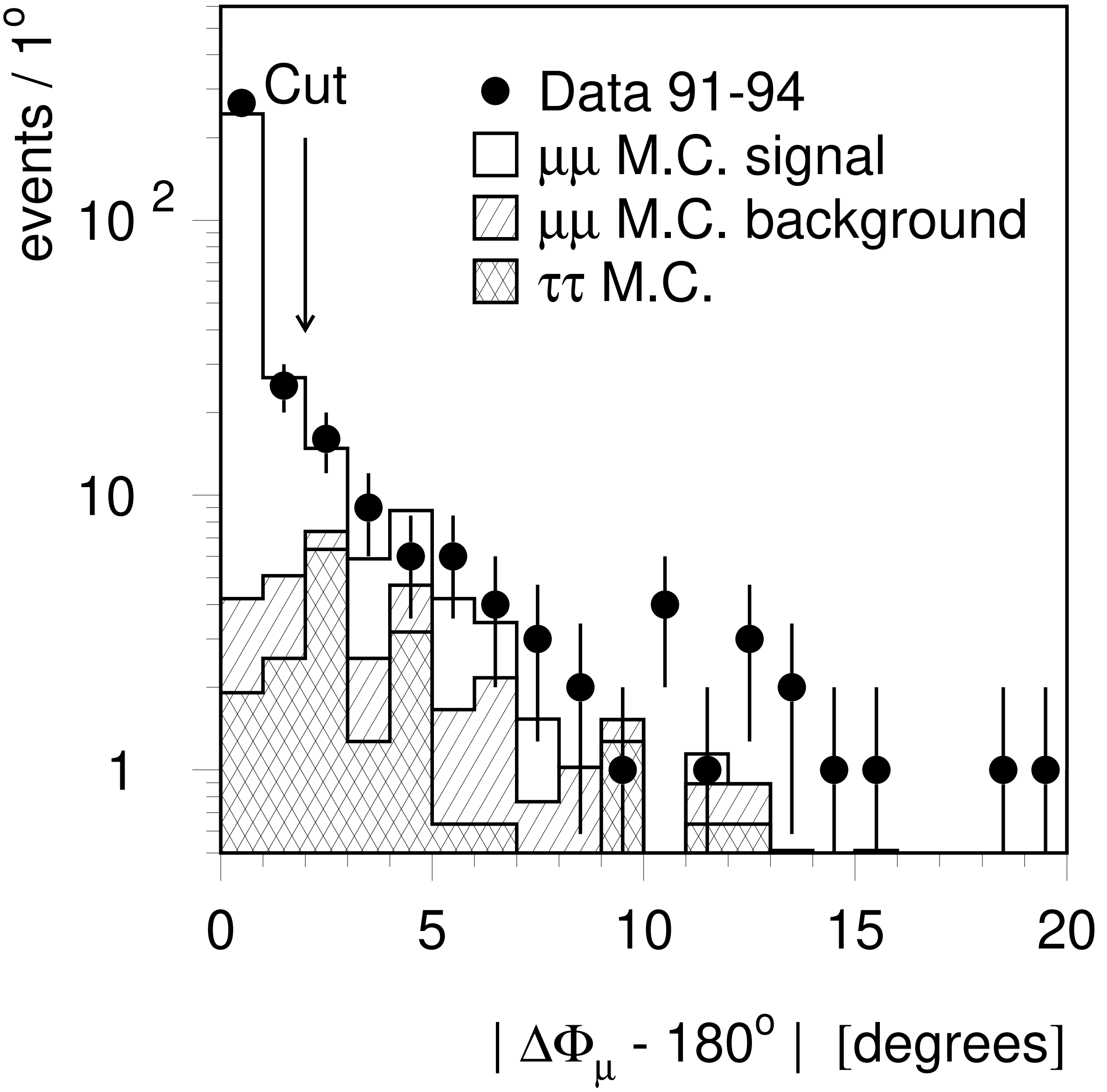

Figure 5: Acoplanarity of the events for data, signal and background Monte Carlo.

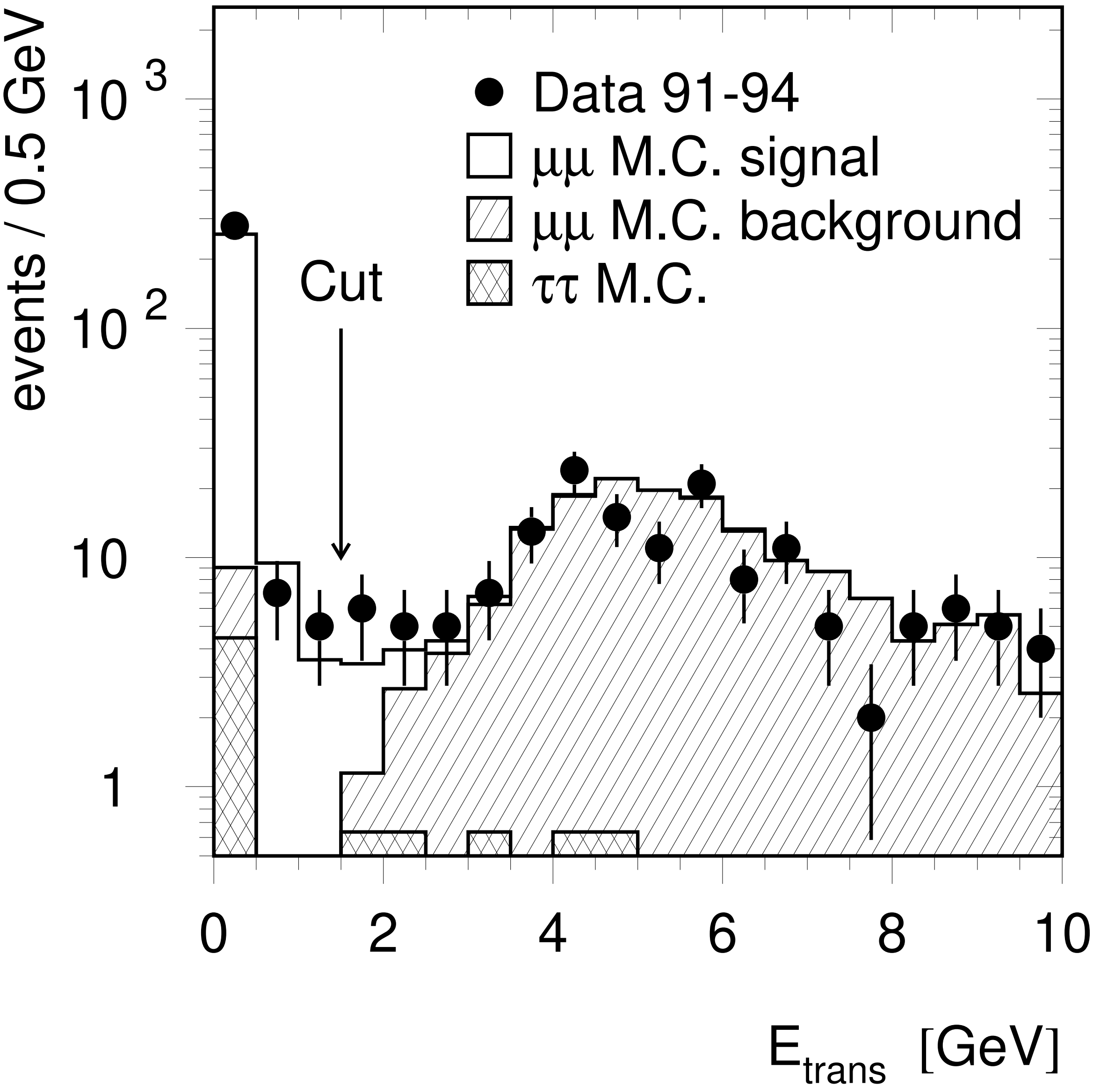

Figure 6: Transverse component of electromagnetic energy to the next muon, E_{trans}, for data, signal and background Monte Carlo.

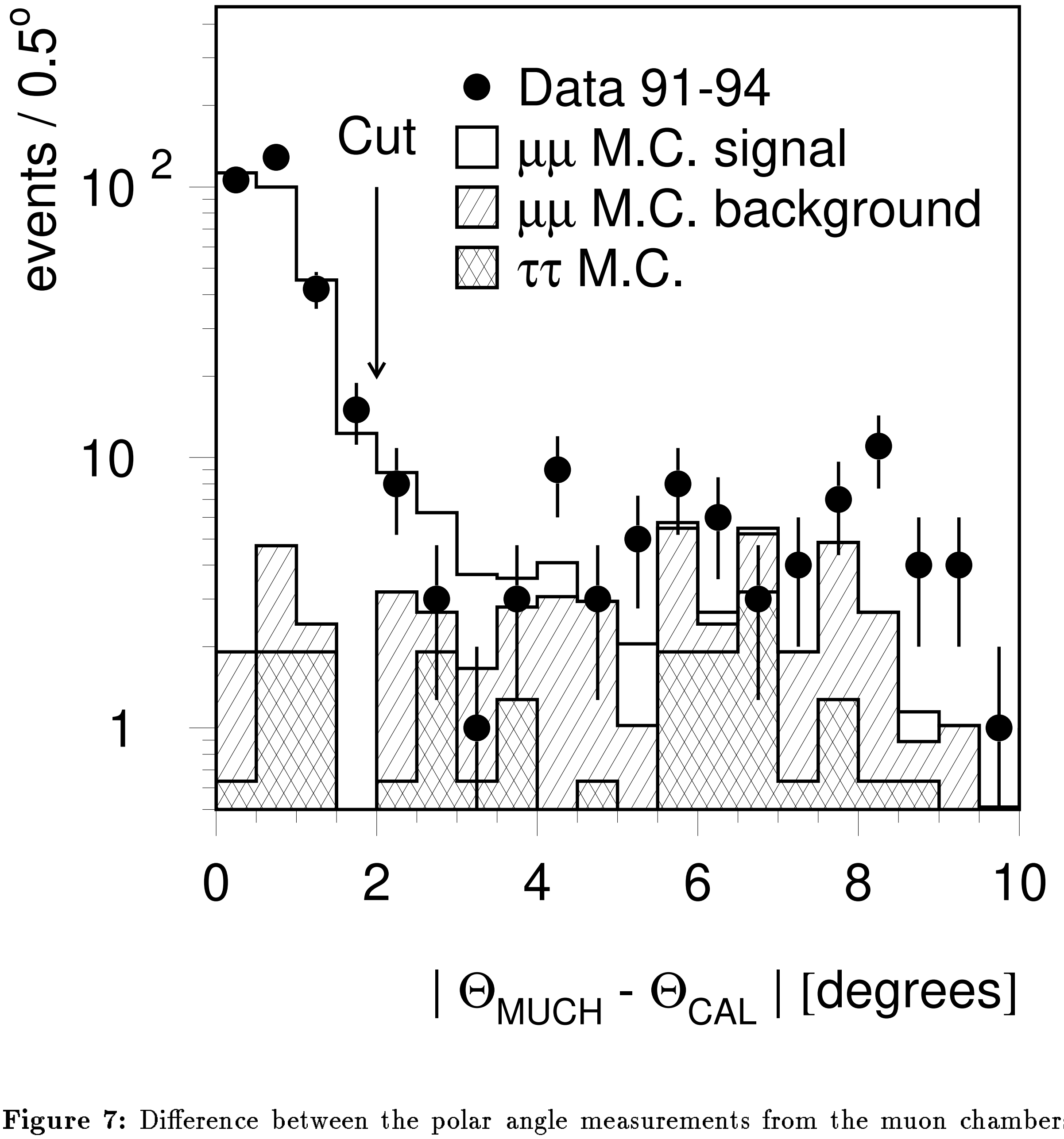

Figure 7: Difference between the polar angle measurements from the muon chambers and from the calorimeter for data, signal and background Monte Carlo.

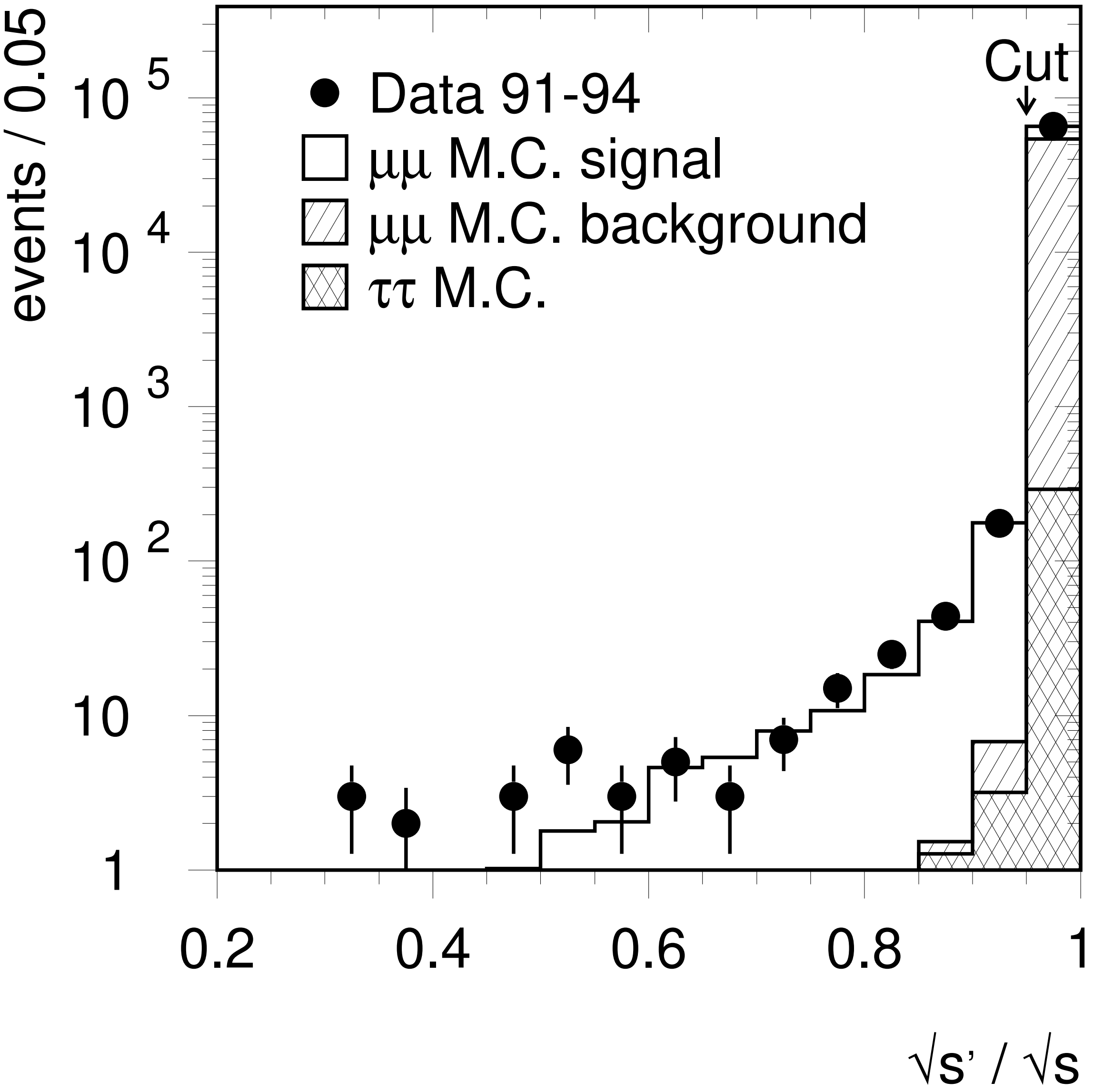

Figure 8: $\sqrt{s'}$ spectrum of the events for data, signal and background Monte Carlo.

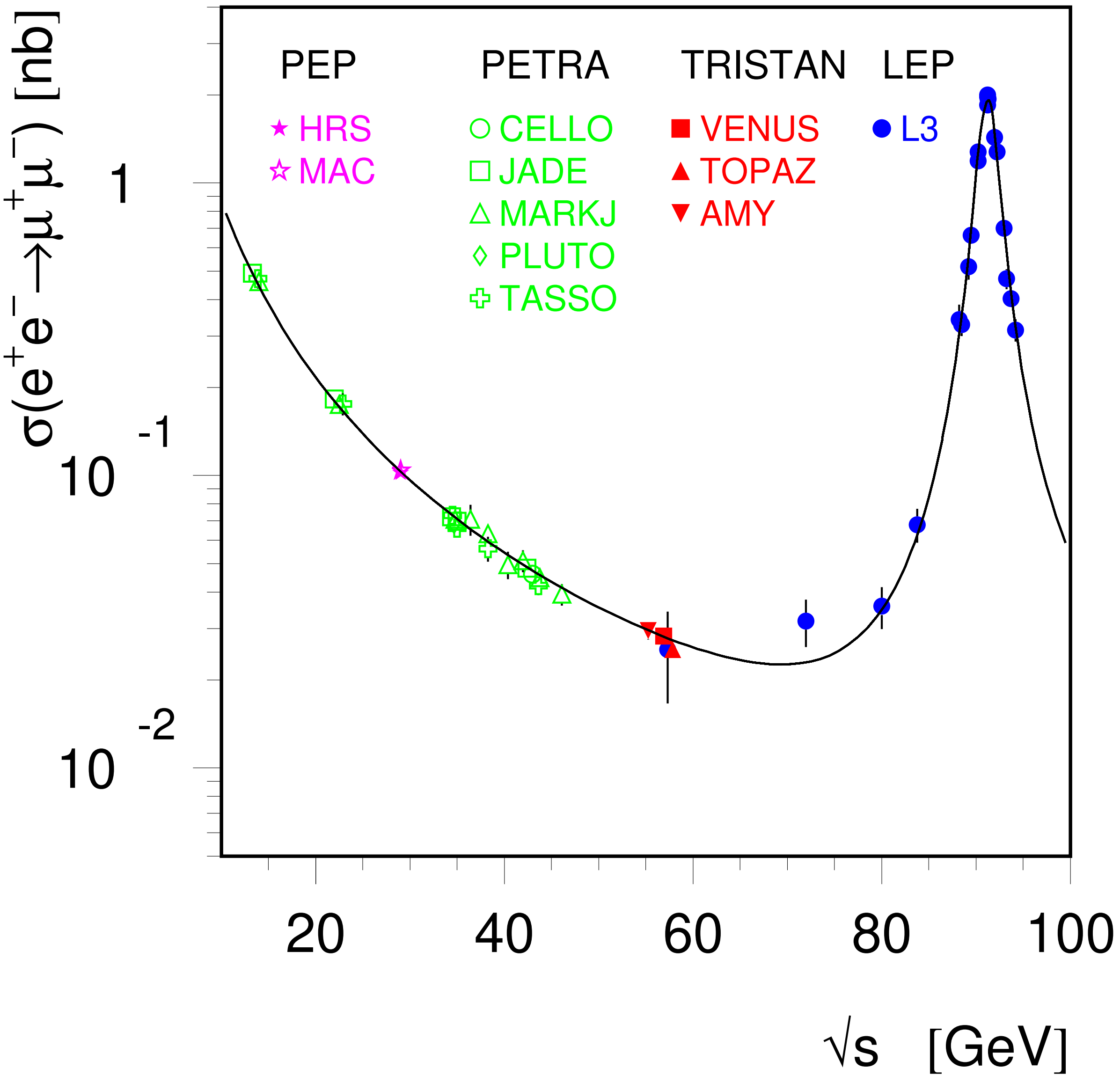

Figure 9: Comparison of the measured cross sections to the lowest order Born prediction and the results of other experiments.

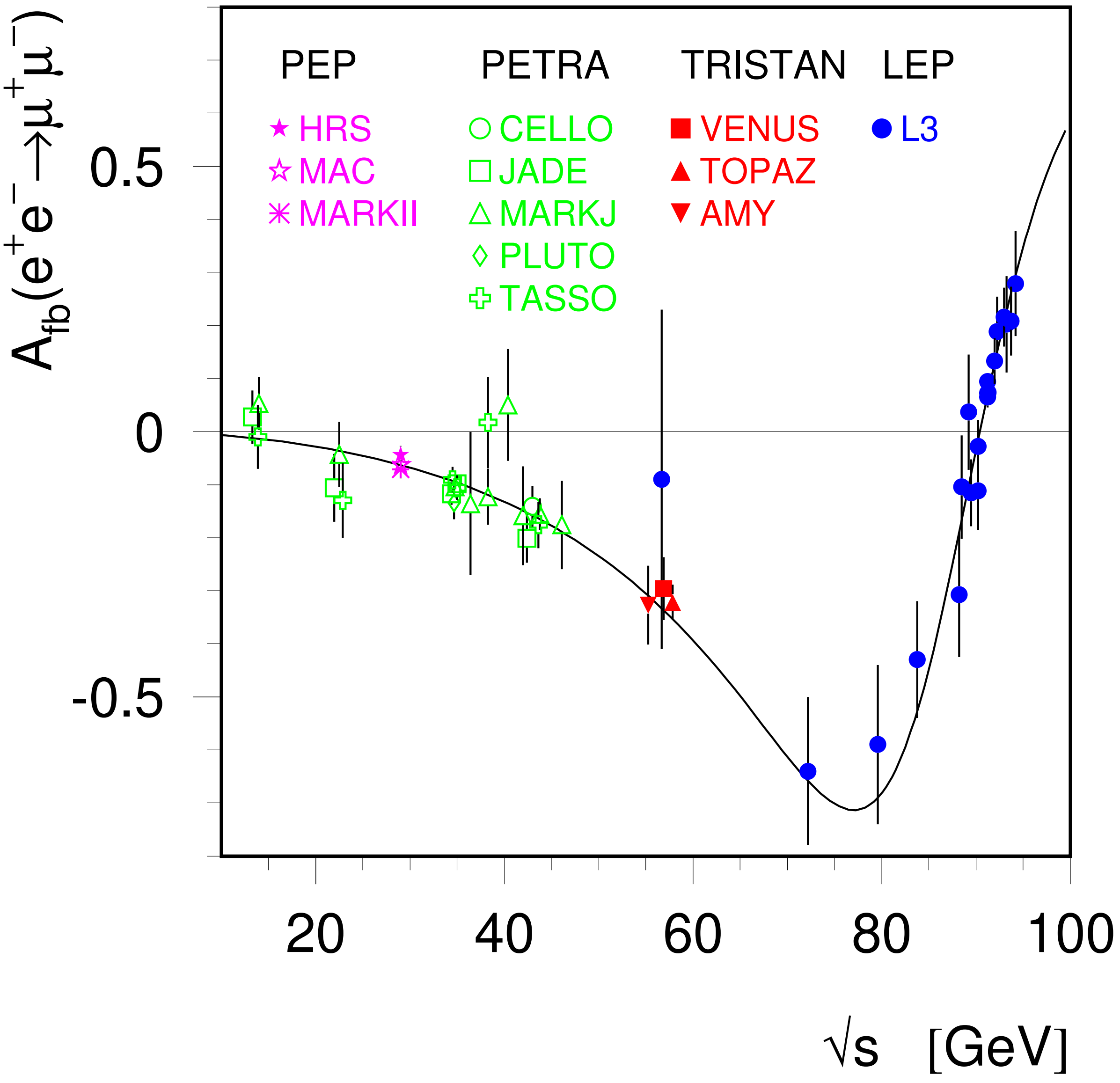

Figure 10: Comparison of measured the forward backward asymmetries to the lowest order Born prediction and the results of other experiments.